Weak lensing of the cosmic microwave background: Power spectrum covariance

Asantha Cooray*
Theoretical Astrophysics, California Institute of Technology, Pasadena, California 91125
(Received 11 October 2001; published 28 February 2002)

We discuss the non-Gaussian contribution to the power spectrum covariance of cosmic microwave background (CMB) anisotropies resulting through weak gravitational lensing angular deflections and the correlation of deflections with secondary sources of temperature fluctuations generated by the large scale structure, such as the integrated Sachs-Wolfe effect and the Sunyaev-Zel'dovich effect. This additional contribution to the covariance of binned angular power spectrum, beyond the well known cosmic variance and any associated instrumental noise, results from a trispectrum, or a four point correlation function, in temperature anisotropy data. With substantially wide bins in multipole space, the resulting non-Gaussian contribution from lensing to the binned power spectrum variance is insignificant out to multipoles of a few thousand and is not likely to affect the cosmological parameter estimation with acoustic peaks and the damping tail. The non-Gaussian contribution to covariance, however, should be considered when interpreting binned CMB power spectrum measurements at multipoles of a few thousand corresponding to angular scales of few arcminutes and less.

DOI: 10.1103/PhysRevD.65.063512 PACS number(s): 98.80.Es, 95.85.Nv

I. INTRODUCTION

The angular power spectrum of cosmic microwave background (CMB) temperature fluctuations, with features such as acoustic peaks and a damping tail [1], is now a well known probe of cosmology [2]; its ability to constrain most, or certain combinations of, parameters that define the currently favorable cold dark matter cosmologies with a cosmological constant has driven a wide number of experiments from ground and space, including the NASA's Microwave Anisotropy Probe (MAP) mission[1] and ESA's planned Planck surveyor.[2] The advent of high sensitivity CMB anisotropy experiments with increasing capabilities to detect fluctuations over a wide range of scales now suggests the possibility that anisotropy power spectrum at small angular scales will soon be measured. At angular scales corresponding to few arcminutes and below, fluctuations are mostly dominated by secondary effects due to local large scale structure (LSS) between us and the recombination. Additionally, important nonlinear second order effects, such as the weak gravitational lensing of CMB [3], leave important imprints that can in return be used as a probe of cosmology or astrophysics related to evolution and growth of structures (e.g., Refs. [4–7]).

The increase in sensitivity of current and upcoming CMB experiments also suggest the possibility that non-Gaussian signals in the CMB temperature fluctuations may be detected and studied in detail [8]. The deviations from Gaussianity in CMB temperature fluctuations arise through two scenarios: the existence of a primordial non-Gaussianity associated with initial fluctuations [9] and the creation of non-Gaussian signals through nonlinear mode-coupling effects related to secondary contributions [4,5]. In currently favored cosmologies with adiabatic initial conditions, the primordial non-Gaussianity is nonexistent or insignificant [9].

This leaves nonlinear mode coupling effects, such as weak lensing of CMB, and gravitational evolution of perturbations at low redshifts as the main sources of non-Gaussianity. Since low redshift secondary effects that trace the nonlinear large scale structure, such as the Sunyaev-Zel'dovich effect [10] due to inverse-Compton scattering of CMB photons via hot electrons, contribute to temperature fluctuations at small angular scales, they act as one of the primary sources of non-Gaussianity in CMB. The existence of non-Gaussian fluctuations in temperature can be directly measured through higher order correlations, such as a three-point function or a bispectrum in Fourier space [4,5]. The detection of non-Gaussianities at the three-point level can be optimized through the use of special statistics and matched filters [11] and through certain physical aspects associated with secondary effects, such as the frequency dependence [12].

Additional effects due to non-Gaussianity include a contribution to the four-point correlation function, or a trispectrum in Fourier space, of CMB temperature fluctuations [13–15]. The four point correlations are of special interest since they quantify the sample variance and covariance of two point correlation or power spectrum measurements [16,17]. Thus, to properly understand the statistical measurements of CMB anisotropy fluctuations at the two point level, a proper understanding of the four point contributions is needed. Similarly, studies of the ability of CMB power spectrum measurements to constrain cosmology [2] have been based on a Gaussian approximation to the sample variance and the assumption that covariance is negligible. If there are significant non-Gaussian contributions from the four point level that contribute to the power spectrum covariance, then it could affect the conversion of power spectrum measurements to estimates on cosmological parameters. Given the high precision level of cosmological parameter measurements expected from CMB, a careful consideration must be attached to understanding the presence of non-Gaussian signals at the four point level. Thus, the basic goal of this paper is to understand to what extent Gaussian assumption on CMB power spectrum covariance remains to hold when non-Gaussian

*Email address: asante@tapir.caltech.edu
[1]http://map.nasa.gsfc.gov
[2]http://astro.estec.esa.nl/Planck/; also, ESA D/SCI(6)3.

contributions are included. As discussed in previous studies (e.g., Refs. [4,5]), one of the most important nonlinear contribution to CMB temperature fluctuations is weak gravitational lensing.

Similar to the weak lensing contribution to CMB anisotropy at the three-point level, the contributions to the four point level results from the nonlinear mode-coupling nature of weak lensing effect and the correlation between weak lensing angular deflections and secondary effects that trace the same large scale structure. The trispectrum due to lensing alone is studied in Ref. [15] and the same trispectrum, under an all-sky formulation, is considered in Ref. [14]. Here, we focus on the contribution of the trispectrum to the power spectrum covariance which was not considered in previous works. We also include the trispectrum resulting from the correlation between lensing and secondary effects such as the integrated Sachs-Wolfe (ISW) [18] effect and the thermal Sunyaev-Zel'dovich (SZ) [10] effect. The latter effect has now been imaged towards massive galaxy clusters where the temperature of the scattering medium can be as high as 10 keV producing temperature fluctuations of order 1 mK [19]. In general, we do not expect secondary contributions such as the thermal SZ effect to be an important non-Gaussian contribution to temperature fluctuations, since its signal can be easily separated from the thermal CMB spectrum based on multifrequency information [12].

Still, we consider the correlation of the SZ effect with lensing as a source of covariance as certain small angular-scale experiments, such as the Cosmic Background Imager [20], may not have the adequate frequency coverage for a proper separation of temperature fluctuation components. In a previous paper, we discussed the non-Gaussian covariance resulting from SZ alone [21], where we also considered the effect of full covariance, compared to Gaussian variance assumption, on the estimation of parameters related to the SZ effect. As discussed there, due to highly non-Gaussian behavior of the SZ signal resulting from its dependence on massive halos such as galaxy clusters, the determination of parameters that define the SZ contribution is significantly affected by the presence of the non-Gaussian contribution to the covariance.

In Sec. II, we introduce the basic ingredients for the present calculation. The CMB anisotropy trispectra due to weak lensing and correlations between weak lensing and secondary effects are derived in Sec. III. In Sec. IV, we calculate the CMB power spectrum covariance due to weak lensing and discuss our results in Sec. V. In Sec. VI we conclude with a summary.

II. GENERAL DERIVATION

Large-scale structure between us and the last scattering surface deflects CMB photons propagating towards us. Since lensing effect on CMB is essentially a distribution of photons, from large scales to small scales, the resulting effect appears only in the second order [14]. In weak gravitational lensing, the deflection angle on the sky is given by the angular gradient of the lensing potential $\alpha(\hat{\mathbf{n}})=\nabla\phi(\hat{\mathbf{n}})$, which itself is a projection of the gravitational potential Φ (see, e.g., [22]),

$$\phi(\hat{\mathbf{m}})=-2\int_0^{r_0}dr\frac{d_A(r_0-r)}{d_A(r)d_A(r_0)}\Phi(r,\hat{\mathbf{m}}r). \tag{1}$$

The quantities here are the conformal distance or look-back time, from the observer, given by

$$r(z)=\int_0^z\frac{dz'}{H(z')}, \tag{2}$$

and the analogous angular diameter distance

$$d_A=H_0^{-1}\Omega_K^{-1/2}\sinh(H_0\Omega_K^{1/2}r), \tag{3}$$

with the expansion rate for adiabatic cold dark matter (CDM) cosmological models with a cosmological constant given by

$$H^2=H_0^2[\Omega_m(1+z)^3+\Omega_K(1+z)^2+\Omega_\Lambda]. \tag{4}$$

Here, H_0 can be written as the inverse Hubble distance today $cH_0^{-1}=2997.9h^{-1}$ Mpc. We follow the conventions that in units of the critical density $3H_0^2/8\pi G$, the contribution of each component is denoted Ω_i, $i=c$ for the CDM, b for the baryons, Λ for the cosmological constant. We also define the auxiliary quantities $\Omega_m=\Omega_c+\Omega_b$ and $\Omega_K=1-\Sigma_i\Omega_i$, which represent the matter density and the contribution of spatial curvature to the expansion rate, respectively. Note that as $\Omega_K\to 0$, $d_A\to r$ and we define $r(z=\infty)=r_0$. Though we present a general derivation of the trispectrum contribution to the covariance, we show results for the currently favorable Λ CDM cosmology with $\Omega_b=0.05$, $\Omega_m=0.35$, $\Omega_\Lambda=0.65$, and $h=0.65$.

The lensing potential in Eq. (1) can be related to the well known convergence generally encountered in conventional lensing studies involving galaxy shear [22]

$$\kappa(\hat{\mathbf{m}})=\frac{1}{2}\nabla^2\phi(\hat{\mathbf{m}})=-\int_0^{r_0}dr\frac{d_A(r)d_A(r_0-r)}{d_A(r_0)}\nabla_\perp^2\Phi(r,\hat{\mathbf{m}}r), \tag{5}$$

where it is noted that the 2D Laplacian operating on Φ is a spatial and not an angular Laplacian. Expanding the lensing potential to Fourier moments

$$\phi(\hat{\mathbf{n}})=\int\frac{d^2\mathbf{l}}{(2\pi)^2}\phi(\mathbf{l})e^{i\mathbf{l}\cdot\hat{\mathbf{n}}}, \tag{6}$$

we can write the usually familiar quantities of convergence and shear components of weak lensing as [14]

$$\kappa(\hat{\mathbf{n}})=-\frac{1}{2}\int\frac{d^2\mathbf{l}}{(2\pi)^2}l^2\phi(\mathbf{l})e^{i\mathbf{l}\cdot\hat{\mathbf{n}}},$$

$$\gamma_1(\hat{\mathbf{n}})\pm i\gamma_2(\hat{\mathbf{n}})=-\frac{1}{2}\int\frac{d^2\mathbf{l}}{(2\pi)^2}l^2\phi(\mathbf{l})e^{\pm i2(\phi_l-\phi)}e^{i\mathbf{l}\cdot\hat{\mathbf{n}}}. \tag{7}$$

Though the two terms κ and ϕ contain differences with respect to radial and wave number weights, these differences cancel with the Limber approximation [23].

The power spectrum of the lensing potential is defined as

$$\langle \phi(\mathbf{l})\phi(\mathbf{l}')\rangle = (2\pi)^2 \delta_D(\mathbf{l}+\mathbf{l}') C_l^{\phi\phi}, \tag{8}$$

where δ_D is the Dirac delta function. Expanding the gravitational potential to density perturbations using the Poisson equation [24]

$$\Phi = \frac{3}{2}\Omega_m \left(\frac{H_0}{k}\right)^2 \left(1+3\frac{H_0^2}{k^2}\Omega_K\right)^{-2} \frac{G(r)}{a}\delta(k,0), \tag{9}$$

we can write the power spectrum of lensing potentials as

$$C_l^{\phi\phi} = \frac{2}{\pi}\int k^2 dk P(k) \int dr_1 W^{\rm len}(k,r_1) j_l(kr_1) \times \int dr_2 W^{\rm len}(k,r_2) j_l(kr_2). \tag{10}$$

Here,

$$W^{\rm len}(k,r) = -3\Omega_m \left(\frac{H_0}{k}\right)^2 \frac{G(r)}{a} \frac{d_A(r_0-r)}{d_A(r) d_A(r_0)} \tag{11}$$

and we have introduced the power spectrum of density fluctuations

$$\langle \delta(\mathbf{k})\delta(\mathbf{k}')\rangle = (2\pi)^3 \delta^{\rm D}(\mathbf{k}+\mathbf{k}') P(k), \tag{12}$$

where

$$\frac{k^3 P(k)}{2\pi^2} = \delta_H^2 \left(\frac{k}{H_0}\right)^{n+3} T^2(k), \tag{13}$$

in linear perturbation theory. We use the fitting formulas of Ref. [25] in evaluating the transfer function $T(k)$ for CDM models. Here, δ_H is the amplitude of present-day density fluctuations at the Hubble scale; with $n=1$, we adopt the Cosmic Background Explorer (COBE) normalization for δ_H [26] of 4.2×10^{-5}, consistent with galaxy cluster abundance [27], with $\sigma_8 = 0.86$. Note that in linear theory, the power spectrum can be scale in time, $P(k,r) = G^2(r) P(k,0)$, using the growth function [28]

$$G(r) \propto \frac{H(r)}{H_0} \int_{z(r)}^{\infty} dz' (1+z') \left(\frac{H_0}{H(z')}\right)^3. \tag{14}$$

In the nonlinear regime, one can use prescriptions such as the fitting function by Ref. [29] to calculate the fully nonlinear density field power spectrum.

Note that an expression of the type in Eq. (10) can be evaluated efficiently with the Limber approximation [23]. Here, we employ a version based on the completeness relation of spherical Bessel functions

$$\int dk k^2 F(k) j_l(kr) j_l(kr') \approx \frac{\pi}{2} d_A^{-2} \delta^{\rm D}(r-r') F(k)\Big|_{k=l/d_A}, \tag{15}$$

where the assumption is that $F(k)$ is a slowly varying function (see Ref. [30] for an alternative approach). Using this, we obtain a useful approximation for the power spectrum of lensing potentials as

$$C_l^{\phi\phi} = \int_0^{r_0} \frac{dr}{d_A^2} \left[W^{\rm len}\left(\frac{l}{d_A}, r\right)\right]^2 P\left(\frac{l}{d_A}; r\right). \tag{16}$$

Note that the power spectrum of convergence is related to that of the potentials via $C_l^{\kappa} = 1/4 l^4 C_l^{\phi\phi}$.

Since the same large scale structure responsible for deflections in CMB photons produces contributions to the anisotropies through other effects, there is a correlation between the deflection potential and secondary sources of temperature fluctuations. As in the power spectrum of deflection potential, using statistical isotropy, we write the correlation as

$$\langle \phi(\mathbf{l})\Theta(\mathbf{l}')^{\rm S}\rangle \equiv (2\pi)^2 \delta_D(\mathbf{l}+\mathbf{l}') b_l^{\rm S} \equiv (2\pi)^2 \delta_D(\mathbf{l}+\mathbf{l}') \frac{-2}{l^2} C_l^{T\kappa}, = \int_0^{r_0} \frac{dr}{d_A^2} W^{\rm S}\left(\frac{l}{d_A}, r\right) W^{\rm len}\left(\frac{l}{d_A}, r\right) P\left(\frac{l}{d_A}; r\right).$$

Here,

$$T^{\rm S}(\hat{\mathbf{n}}) = \int \frac{d^2\mathbf{l}}{(2\pi)^2} \Theta(\mathbf{l}) \tag{17}$$

and we have used Eq. (7) to relate the power spectrum $b_l^{\rm S}$ of Refs. [4,5] and the κ-secondary cross power spectrum of Ref. [31]. The last line again represents the Limber approximation, similar to the derivation of the lensing potential power spectrum in Eq. (16).

In the present paper we consider two secondary effects that correlate with lensing deflections: integrated Sachs-Wolfe effect and the Sunyaev-Zel'dovich effect. At small angular scales, the lensing signal in CMB data can also correlate with other secondary effects due to large scale structure. In an experiment where frequency separation allows the extraction of the SZ signal, the non-Gaussian contribution in the CMB component will likely come from the correlation between the lensing effect and a source of secondary anisotropy. At small angular scales, other sources of secondary effects depend on the velocity field of electrons. The cross correlation of lensing and contributions due to linear velocity terms, such as the linear Doppler effect or the kinetic SZ effect due to density modulation of the velocity field [33,10], is significantly suppressed due to positive-negative cancellations arising from the velocity fluctuations [32]. Thus, after the SZ effect, the next significant secondary-lensing correlation results from effects which depends on the velocity with

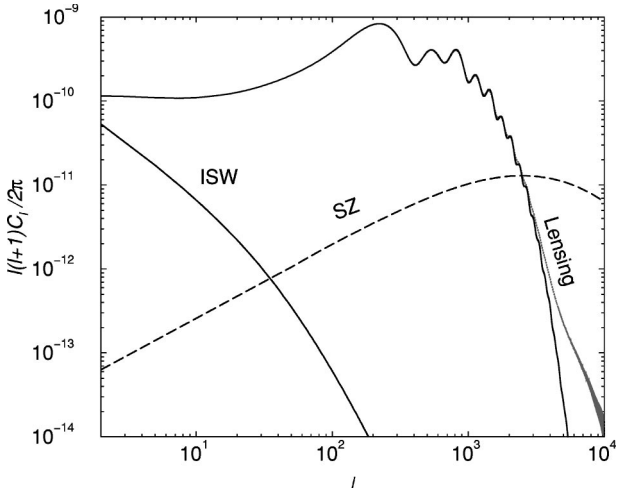

FIG. 1. Power spectrum of the CMB temperature anisotropies in the fiducial Λ CDM model. We have also shown the weak lensing, integrated Sachs-Wolfe and the SZ secondary contributions to angular power spectrum.

a quadratic term. These correlations are at least three orders of magnitude smaller than the lensing-SZ correlation and are not likely to be a significant source of non-Gaussianity. As we find out later, even if the SZ effect is removed through spectral information in CMB data, the lensing effect alone produces a significant non-Gaussianity at multipoles of a few thousand and this contribution is likely to be more relevant for present and upcoming CMB experiments at arcminute scales.

The ISW [18] effect results from the late time decay of gravitational potential fluctuations and its contribution to temperature dominates at large angular scales (see Fig. 1). The resulting temperature fluctuations in the CMB can be written as

$$T^{\rm ISW}(\hat{\mathbf{n}}) = -2\int_0^{r_0} dr \dot{\Phi}(r,\hat{\mathbf{n}}r). \tag{18}$$

The weight function associated with the ISW effect is given by

$$W^{\rm ISW}(k) = -3\Omega_m \left(\frac{H_0}{k}\right)^2 \dot{F}(r), \tag{19}$$

which can be used to calculated the correlation between lensing potential and the ISW effect through Eq. (17).

The SZ effect leads to an effective temperature fluctuation in the CMB given by the integrated pressure fluctuation along the line of sight

$$T^{\rm SZ}(\hat{\mathbf{n}}) = g(x)\int dr a(r) \frac{k_B \sigma_T}{m_e c^2} n_e(r) T_e(r), \tag{20}$$

where σ_T is the Thomson cross section, n_e is the electron number density, r is the comoving distance, and $g(x) = x\coth(x/2) - 4$ with $x = h\nu/k_B T_{\rm CMB}$ the spectral shape of the SZ effect. At the Rayleigh-Jeans (RJ) part of the CMB, $g(x) = -2$. For the rest of this paper, we assume observations in the Rayleigh-Jeans regime of the spectrum; an experiment such as Planck with sensitivity beyond the peak of the spectrum can separate out SZ contributions based on the spectral signature $g(x)$ [12]. At the RJ part of the frequency spectrum, the SZ weight function is

$$W^{\rm SZ}(r) = -2\frac{k_B \sigma_T \bar{n}_e}{a(r)^2 m_e c^2}, \tag{21}$$

where $\bar{n}_e$ is the mean electron density today.

For the correlation between lensing and the SZ effect, we follow the halo model approach of Ref. [34] (see Ref. [35] for further details) which allows a semianalytical approach to calculate the power spectrum of large scale structure pressure fluctuations. With the halo model, we replace the clustering of dark matter with that of pressure when describing the SZ effect. The cross correlation between lensing and SZ then involves the cross-power spectrum between pressure and dark matter which is discussed in detail in [34,21], to which we refer the reader for further details.

The basic assumption of the halo model is that large scale structure dark matter distribution can be viewed as a collection of dark matter halos with a mass function following Press-Schechter [36] mass function or variants and a dark matter distribution in each halo following the Navarro-Frenk-White (NFW) profile of [37] or similar descriptions. The halos are distributed such that they trace the linear density field with a bias described in Ref. [38]. With clustering of dark matter described through such an approach, any other physical property of the large scale structure can be easily described through the relation between the property of interest and the dark matter. For example, in the case of pressure necessary for the description of the SZ effect, the gas distribution in each halo is assumed to follow hydrostatic equilibrium with dark matter distribution. As discussed in Ref. [34], the approach based on halos provides a reliable semianalytical approach to model nonlinear large scale structure clustering. The predictions based on the halo model, as relevant for the SZ effect and lensing-SZ correlations, are consistent with numerical simulations (e.g., Ref. [39]).

In Fig. 1, we show the angular power spectrum of CMB anisotropies [40] with secondary contributions through weak lensing, ISW and SZ effects. The SZ angular power spectrum was calculated using the halo approach of Ref. [34]. The lensing angular deflection power spectrum and the resulting correlation power spectra between lensing and ISW, and, lensing and SZ effects are shown in Fig. 2.

III. LENSING CONTRIBUTION TO CMB

In order to derive weak lensing contributions to the CMB trispectrum, we follow Hu [14] and Zaldarriaga [15]. We formulate the contribution under a flat sky approximation; this formulation is adequate given that we are mostly interested in non-Gaussian effects due to lensing at small angular scales corresponding to multipoles $\gtrsim 1000$. In general, the flat-sky approach simplifies the derivation and computation

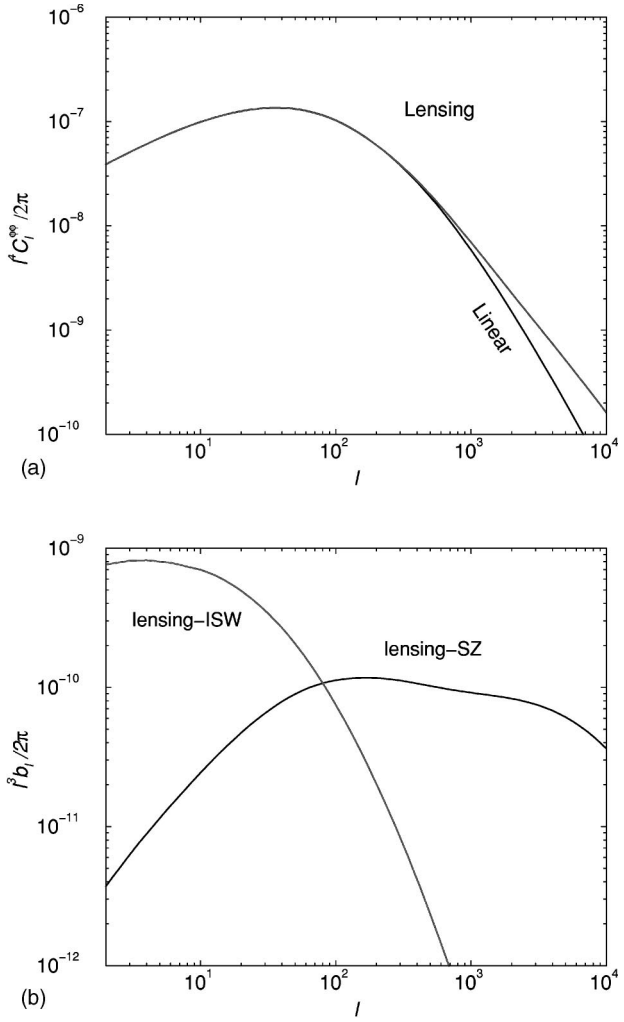

FIG. 2. Power spectra of (a) lensing angular deflections and (b) lensing-ISW and lensing-SZ cross-correlation. In (a), we show the lensing deflection power spectrum under linear perturbation theory description of the matter fluctuations and using the halo model. As shown, the lensing deflection power peaks at multipoles of ~ 40 and act as an effective window function which smoothes the CMB power spectrum. In (b), the lensing-SZ correlation is calculated with the halo approach while lensing-ISW correlation follows the use of linear theory dark matter power spectrum.

through the replacement of mode-coupling Wigner symbols through angles.

As discussed in prior papers [4,5,14], weak lensing maps temperature through the angular deflections resulting along the photon path by

$$\Theta^{\rm t}(\hat{\mathbf{n}}) = \Theta(\hat{\mathbf{n}} + \nabla\phi) = \Theta(\hat{\mathbf{n}}) + \nabla_i \phi(\hat{\mathbf{n}}) \nabla^i \Theta(\hat{\mathbf{n}}) + \frac{1}{2}\nabla_i\phi(\hat{\mathbf{n}})\nabla_j\phi(\hat{\mathbf{n}})\nabla^i\nabla^j\Theta(\hat{\mathbf{n}}) + \cdots . \quad (22)$$

As expected for lensing, note that the remapping conserves the surface brightness distribution of CMB. Here, $\Theta(\hat{\mathbf{n}})$ is the unlensed primary component of CMB and $\Theta^{\rm t}(\hat{\mathbf{n}})$ is the total contribution. It should be understood that in the presence of low redshift contributions to CMB resulting through large scale structure, the total contribution includes a secondary contribution which we denote by $\Theta^{\rm s}(\hat{\mathbf{n}})$. Since weak lensing deflection angles also trace the large scale structure at low redshifts, secondary effects which are first order in density or potential fluctuations also correlate with the lensing deflection angle ϕ.

Taking the Fourier transform, as appropriate for a flat sky, we write

$$\tilde{\Theta}(\mathbf{l}_1) = \int d\hat{\mathbf{n}} \tilde{\Theta}(\hat{\mathbf{n}}) e^{-i\mathbf{l}_1\cdot\hat{\mathbf{n}}} = \Theta(\mathbf{l}_1) - \int \frac{d^2\mathbf{l}_1'}{(2\pi)^2}\Theta(\mathbf{l}_1')L(\mathbf{l}_1,\mathbf{l}_1'), \quad (23)$$

where

$$L(\mathbf{l}_1,\mathbf{l}_1') = \phi(\mathbf{l}_1-\mathbf{l}_1')(\mathbf{l}_1-\mathbf{l}_1')\cdot\mathbf{l}_1' + \frac{1}{2}\int \frac{d^2\mathbf{l}_1''}{(2\pi)^2}\phi(\mathbf{l}_1'')\phi^*(\mathbf{l}_1''+\mathbf{l}_1'-\mathbf{l}_1)(\mathbf{l}_1''\cdot\mathbf{l}_1') \times(\mathbf{l}_1''+\mathbf{l}_1'-\mathbf{l}_1)\cdot\mathbf{l}_1'. \quad (24)$$

We define the power spectrum and the trispectrum in the flat sky approximation following the usual way:

$$\langle\Theta^{\rm t}(\mathbf{l}_1)\Theta^{\rm t}(\mathbf{l}_2)\rangle = (2\pi)^2\delta_{\rm D}(\mathbf{l}_{12})\tilde{C}_l^\Theta, \quad \langle\Theta^{\rm t}(\mathbf{l}_1)\ldots\Theta^{\rm t}(\mathbf{l}_4)\rangle_c = (2\pi)^2\delta_{\rm D}(\mathbf{l}_{1234})\tilde{T}^\Theta(\mathbf{l}_1,\mathbf{l}_2,\mathbf{l}_3,\mathbf{l}_4). \quad (25)$$

A. Power spectrum

The power spectrum, according to the present formulation, is discussed in Ref. [14] and we can write

$$\tilde{C}_l^\Theta = \left[1 - \int \frac{d^2\mathbf{l}_1}{(2\pi)^2} C_{l_1}^{\phi\phi}(\mathbf{l}_1\cdot\mathbf{l})^2\right] C_l^\Theta + \int \frac{d^2\mathbf{l}_1}{(2\pi)^2} C^\Theta_{|\mathbf{l}-\mathbf{l}_1|} C_{l_1}^{\phi\phi}[(\mathbf{l}-\mathbf{l}_1)\cdot\mathbf{l}_1]^2. \quad (26)$$

As written, the second term shows the smoothing behavior of weak lensing through a convolution [Eq. (26)] of the CMB power spectrum (see discussion in Ref. [14]). With respect to lensing contribution, there are two limiting cases: when $\mathbf{l}-\mathbf{l}_1 \approx \mathbf{l}$ and CMB power is constant, one can take the CMB power spectrum out of the integral in the second term such that

$$\tilde{C}_l^\Theta \approx \left[1 - \int \frac{d^2\mathbf{l}_1}{(2\pi)^2} C_{l_1}^{\phi\phi}(\mathbf{l}_1\cdot\mathbf{l})^2\right] C_l^\Theta + C_l^\Theta \int \frac{d^2\mathbf{l}_1}{(2\pi)^2} C_{l_1}^{\phi\phi}(\mathbf{l}\cdot\mathbf{l}_1)^2. \quad (27)$$

Thus, there is a net cancellation of terms involving lensing potential power spectrum and $\tilde{C}_l^\Theta \approx C_l^\Theta$ producing the well known result that lensing shifts but does not create power on large scales [14]. On small scales where there is little or no intrinsic power in the CMB, the second term behaves such that

$$\tilde{C}_l^\Theta \approx \frac{1}{2} l^2 C_l^{\phi\phi} \int \frac{d^2\mathbf{l}_1}{(2\pi)^2} l_1^2 C_{l_1}^\Theta. \tag{28}$$

Here, the power generated is effectively the lensing of the temperature gradient associated with the damping tail of CMB anisotropy power spectrum. This small angular scale limit and its uses as a probe of large scale structure density power spectrum and mass distribution of collapsed halos such as galaxy clusters is considered in Ref. [42].

B. Trispectrum

The calculation of the trispectrum follows similar to the power spectrum. Here, we explicitly show the calculation for one term of the trispectrum and add all other terms through permutations. First we consider the cumulants involving four temperature terms in Fourier space:

$$\begin{aligned}
\langle \Theta^{\mathrm{t}}(\mathbf{l}_1)\cdots\Theta^{\mathrm{t}}(\mathbf{l}_4)\rangle_c &\left\langle \left(\Theta(\mathbf{l}_1) - \int \frac{d^2\mathbf{l}_1'}{(2\pi)^2} \Theta(\mathbf{l}_1') L(\mathbf{l}_1,\mathbf{l}_1') \right) \right. \\
&\left. \times \left(\Theta(\mathbf{l}_2) - \int \frac{d^2\mathbf{l}_2'}{(2\pi)^2} \Theta(\mathbf{l}_2') L(\mathbf{l}_2,\mathbf{l}_2') \right) \Theta(\mathbf{l}_3)\Theta(\mathbf{l}_4) \right\rangle \\
&= \left\langle \int \frac{d^2\mathbf{l}_1'}{(2\pi)^2} \Theta(\mathbf{l}_1') L(\mathbf{l}_1,\mathbf{l}_1') \right. \\
&\left. \times \int \frac{d^2\mathbf{l}_2'}{(2\pi)^2} \Theta(\mathbf{l}_2') L(\mathbf{l}_2,\mathbf{l}_2') \Theta(\mathbf{l}_3)\Theta(\mathbf{l}_4) \right\rangle .
\end{aligned} \tag{29}$$

As written, to the lowest order, we find that contributions come from the first order term in L given in Eq. (24). We further simplify to obtain

$$\begin{aligned}
\langle \Theta^{\mathrm{t}}(\mathbf{l}_1)\cdots\Theta^{\mathrm{t}}(\mathbf{l}_4)\rangle_c = &\left\langle \int \frac{d^2\mathbf{l}_1'}{(2\pi)^2} \Theta(\mathbf{l}_1')\, \phi(\mathbf{l}_1-\mathbf{l}_1')(\mathbf{l}_1 \right. \\
&-\mathbf{l}_1')\cdot\mathbf{l}_1' \int \frac{d^2\mathbf{l}_2'}{(2\pi)^2} \Theta(\mathbf{l}_2')\, \phi(\mathbf{l}_2-\mathbf{l}_2') \\
&\left. \times(\mathbf{l}_2-\mathbf{l}_2')\cdot\mathbf{l}_2' \Theta(\mathbf{l}_3)\Theta(\mathbf{l}_4) \right\rangle \\
&= C_{l_3}^\Theta C_{l_4}^\Theta \langle \phi(\mathbf{l}_1+\mathbf{l}_3)\, \phi(\mathbf{l}_2+\mathbf{l}_4)\rangle (\mathbf{l}_1 \\
&+\mathbf{l}_3)\cdot\mathbf{l}_3(\mathbf{l}_2+\mathbf{l}_4)\cdot\mathbf{l}_4 + \mathrm{Perm.},
\end{aligned} \tag{30}$$

where there is an additional term through a permutation involving the interchange of $\mathbf{l}_1+\mathbf{l}_3$ with $\mathbf{l}_1+\mathbf{l}_4$. Introducing the power spectrum of lensing potentials, we further simplify to obtain the CMB trispectrum due to gravitational lensing:

$$\begin{aligned}
\tilde{T}^\Theta(\mathbf{l}_1,\mathbf{l}_2,\mathbf{l}_3,\mathbf{l}_4) = &- C_{l_3}^\Theta C_{l_4}^\Theta [C_{|\mathbf{l}_1+\mathbf{l}_3|}^{\phi\phi} (\mathbf{l}_1+\mathbf{l}_3)\cdot\mathbf{l}_3 (\mathbf{l}_1+\mathbf{l}_3)\cdot\mathbf{l}_4 \\
&+ C_{|\mathbf{l}_2+\mathbf{l}_3|}^{\phi\phi} (\mathbf{l}_2+\mathbf{l}_3)\cdot\mathbf{l}_3 (\mathbf{l}_2+\mathbf{l}_3)\cdot\mathbf{l}_4] + \mathrm{Perm.},
\end{aligned} \tag{31}$$

where the permutations now contain 5 additional terms with the replacement of (l_3, l_4) pair by other combinations of the pairs.

The trispectrum, through coupling of lensing deflection angle to secondary effects, can be calculated with the replacement of $\Theta(\mathbf{l}_3)$ and $\Theta(\mathbf{l}_4)$ in Eq. (29) by $\Theta^{\mathrm{S}}(\mathbf{l}_3)$ and $\Theta^{\mathrm{S}}(\mathbf{l}_4)$ containing the sources of secondary fluctuations. Thus, we can no longer consider cumulants such as $\langle \Theta(\mathbf{l}_1')\Theta^{\mathrm{S}}(\mathbf{l}_3)\rangle$ as the secondary effects are decoupled from recombination where primary fluctuations are imprinted. However, contributions come from the correlation between Θ^{S} and the lensing deflection ϕ. Here, contributions of equal importance come from both the first and second order terms in L written in Eq. (24). First, we note

$$\begin{aligned}
\langle \Theta(\mathbf{l}_1)\cdots\Theta(\mathbf{l}_4)\rangle_c = &\left\langle \left(\Theta(\mathbf{l}_1) - \int \frac{d^2\mathbf{l}_1'}{(2\pi)^2} \Theta(\mathbf{l}_1') L(\mathbf{l}_1,\mathbf{l}_1') \right) \right. \\
&\times \left(\Theta(\mathbf{l}_2) - \int \frac{d^2\mathbf{l}_2'}{(2\pi)^2} \Theta(\mathbf{l}_2') L(\mathbf{l}_2,\mathbf{l}_2') \right) \\
&\left. \times \Theta^s(\mathbf{l}_3)\Theta^s(\mathbf{l}_4) \right\rangle \\
= &- C_{l_1} \langle L(\mathbf{l}_2,-\mathbf{l}_1)\Theta^s(\mathbf{l}_3)\Theta^s(\mathbf{l}_4)\rangle \\
&- C_{l_2} \langle L(\mathbf{l}_1,-\mathbf{l}_2)\Theta^s(\mathbf{l}_3)\Theta^s(\mathbf{l}_4)\rangle \\
&+ \int \frac{d^2\mathbf{l}_1'}{(2\pi)^2} C_{l_1'} \langle L(\mathbf{l}_2, \\
&-\mathbf{l}_1') L(\mathbf{l}_1,\mathbf{l}_1')\Theta^s(\mathbf{l}_3)\Theta^s(\mathbf{l}_4)\rangle .
\end{aligned} \tag{32}$$

Contributions to the trispectrum from the first two terms come through the second order term in L, with the two ϕ terms coupling to Θ^s. In the last term, contributions come from the first order term of L similar to the lensing alone contribution to trispectrum.

After some straightforward simplifications, we write the connected part of the trispectrum involving lensing-secondary coupling as

$$\begin{aligned}
\tilde{T}^\Theta(\mathbf{l}_1,\mathbf{l}_2,\mathbf{l}_3,\mathbf{l}_4) = &- C_{l_3}^{\phi\mathrm{s}} C_{l_4}^{\phi\mathrm{s}} [C_{l_1}^\Theta (\mathbf{l}_3\cdot\mathbf{l}_1)(\mathbf{l}_4\cdot\mathbf{l}_1) + C_{l_2}^\Theta (\mathbf{l}_3\cdot\mathbf{l}_2) \\
&\times (\mathbf{l}_4\cdot\mathbf{l}_2) + \mathbf{l}_3\cdot(\mathbf{l}_1+\mathbf{l}_3)\mathbf{l}_4\cdot(\mathbf{l}_2+\mathbf{l}_4) C_{l_{13}}^\Theta \\
&+ \mathbf{l}_4\cdot(\mathbf{l}_1+\mathbf{l}_4)\mathbf{l}_3\cdot(\mathbf{l}_2+\mathbf{l}_3) C_{l_{14}}^\Theta] + \mathrm{Perm.}
\end{aligned} \tag{33}$$

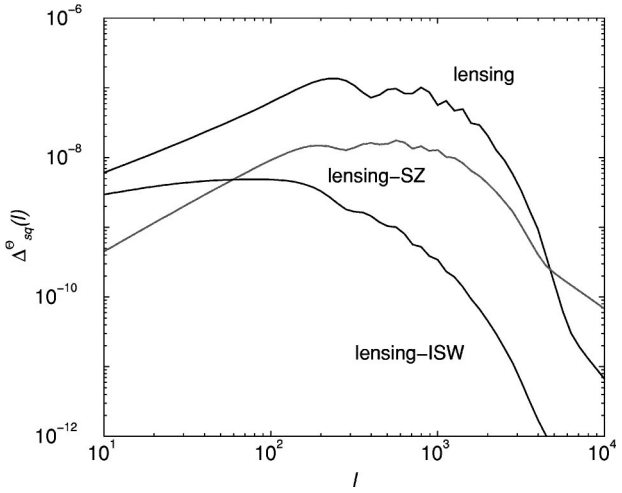

FIG. 3. CMB anisotropy trispectrum resulting from lensing, lensing-ISW and lensing-SZ correlations. The lensing trispectrum generally follows the shape of the CMB power spectrum while lensing-ISW and lensing-SZ trispectra depict the behavior of correlation power between lensing and these secondary effects.

Note that the first two terms come from the first and second terms in Eq. (32), while the last two terms in the above are from the third term. As before, through permutations, there are five additional terms involving the pairings of (l_3, l_4).

IV. POWER SPECTRUM COVARIANCE

For the purpose of this calculation, we assume that CMB power spectrum will measure binned logarithmic band powers at several l_i's in multipole space with bins of thickness δl_i.

$$\mathcal{C}_i = \int_{si} \frac{d^2l}{A_{si}} \frac{l^2}{2\pi} \Theta(\mathbf{l})\Theta(-\mathbf{l}), \tag{34}$$

where $A_s(l_i) = \int d^2l$ is the area of 2D shell in multipole and can be written as $A_s(l_i) = 2\pi l_i \delta l_i + \pi(\delta l_i)^2$.

We can now write the signal covariance matrix as

$$C_{ij} = \frac{1}{A}\left[\frac{(2\pi)^2}{A_{si}} 2\mathcal{C}_i^2 + T^{\Theta}_{ij}\right], \tag{35}$$

$$T^{\Theta}_{ij} = \int \frac{d^2l_i}{A_{si}} \int \frac{d^2l_j}{A_{sj}} \frac{l_i^2 l_j^2}{(2\pi)^2} T^{\Theta}(\mathbf{l}_i, -\mathbf{l}_i, \mathbf{l}_j, -\mathbf{l}_j), \tag{36}$$

where A is the area of the survey in steradians. Again the first term is the Gaussian contribution to the sample variance and includes, in addition to the primary component, the contribution through lensing and secondary effects. The second term is the non-Gaussian contribution. A realistic survey will also include instrumental noise contributions and we can modify the Gaussian variance to include the noise through an additional noise contribution to the power spectrum

$$C_l^{\mathrm{t}} = C_l^{\Theta} + N_l, \tag{37}$$

where N_l is the power spectrum of the detector and other sources of noise introduced by the experiment.

For the power spectrum covariance, we are interested in the case when $\mathbf{l}_2 = -\mathbf{l}_1$ with $|\mathbf{l}_1| = l_i$ and $\mathbf{l}_4 = -\mathbf{l}_3$ with $|\mathbf{l}_3| = l_j$. This denotes parallelograms for the trispectrum configuration in multipolar or Fourier space.

In the case of the lensing contribution to the trispectrum, with the configuration required for the power spectrum covariance, we can write

$$\begin{aligned} T^{\Theta}(\mathbf{l}_i, -\mathbf{l}_i, \mathbf{l}_j, -\mathbf{l}_j) = {} & C^{\Theta}_{l_i} C^{\Theta}_{l_i} [C^{\phi\phi}_{|\mathbf{l}_i+\mathbf{l}_j|} [(\mathbf{l}_i+\mathbf{l}_j)\cdot\mathbf{l}_i]^2 + C^{\phi\phi}_{|\mathbf{l}_i-\mathbf{l}_j|} [(\mathbf{l}_i \\ & -\mathbf{l}_j)\cdot\mathbf{l}_i]^2] + C^{\Theta}_{l_j} C^{\Theta}_{l_j} [C^{\phi\phi}_{|\mathbf{l}_i+\mathbf{l}_j|} [(\mathbf{l}_i+\mathbf{l}_j)\cdot\mathbf{l}_j]^2 \\ & + C^{\phi\phi}_{|\mathbf{l}_i-\mathbf{l}_j|} [(\mathbf{l}_i-\mathbf{l}_j)\cdot\mathbf{l}_j]^2] \\ & + 2 C^{\Theta}_{l_i} C^{\Theta}_{l_j} [C^{\phi\phi}_{|\mathbf{l}_i+\mathbf{l}_j|} (\mathbf{l}_i+\mathbf{l}_j)\cdot\mathbf{l}_i (\mathbf{l}_i+\mathbf{l}_j)\cdot\mathbf{l}_j \\ & - C^{\phi\phi}_{|\mathbf{l}_i-\mathbf{l}_j|} (\mathbf{l}_i-\mathbf{l}_j)\cdot\mathbf{l}_i (\mathbf{l}_i-\mathbf{l}_j)\cdot\mathbf{l}_j], \end{aligned} \tag{38}$$

which includes all terms with no additional permutations.

Similarly, for the lensing-secondary trispectrum we have

$$\begin{aligned} T^{\Theta}(\mathbf{l}_i, -\mathbf{l}_i, \mathbf{l}_j, -\mathbf{l}_j) = {} & 2(\mathbf{l}_i\cdot\mathbf{l}_j)^2 [(C^{\phi s}_{l_i})^2 C^{\Theta}_{l_j} + (C^{\phi s}_{l_j})^2 C^{\Theta}_{l_i}] \\ & - [[\mathbf{l}_i\cdot(\mathbf{l}_i+\mathbf{l}_j)]^2 (C^{\phi s}_{l_i})^2 + [\mathbf{l}_j\cdot(\mathbf{l}_i+\mathbf{l}_j)]^2 \\ & \times (C^{\phi s}_{l_j})^2] C^{\Theta}_{|\mathbf{l}_i+\mathbf{l}_j|} - [[\mathbf{l}_i\cdot(\mathbf{l}_i-\mathbf{l}_j)]^2 (C^{\phi s}_{l_i})^2 \\ & + [\mathbf{l}_j\cdot(\mathbf{l}_i-\mathbf{l}_j)]^2 (C^{\phi s}_{l_j})^2] C^{\Theta}_{|\mathbf{l}_i-\mathbf{l}_j|} \\ & + 2[\mathbf{l}_i\cdot(\mathbf{l}_j-\mathbf{l}_i)][\mathbf{l}_j\cdot(\mathbf{l}_j-\mathbf{l}_i)] \\ & \times C^{\phi s}_{l_i} C^{\phi s}_{l_j} C^{\Theta}_{|\mathbf{l}_j-\mathbf{l}_i|} - 2[\mathbf{l}_i\cdot(\mathbf{l}_i+\mathbf{l}_j)] \\ & \times [\mathbf{l}_j\cdot(\mathbf{l}_i+\mathbf{l}_j)] C^{\phi s}_{l_i} C^{\phi s}_{l_j} C^{\Theta}_{|\mathbf{l}_i+\mathbf{l}_j|}. \end{aligned} \tag{39}$$

V. RESULTS

In Fig. 3, we show the scaled trispectra, where

$$\Delta^{\Theta}_{\mathrm{sq}}(l) = \frac{l^2}{2\pi} T^{\Theta}(\mathbf{l}, -\mathbf{l}, \mathbf{l}_\perp, -\mathbf{l}_\perp)^{1/3} \tag{40}$$

and $l_\perp = l$ and $\mathbf{l}\cdot\mathbf{l}_\perp = 0$. In the case of lensing alone, the trispectrum is proportional to the square of the CMB anisotropy power spectrum [see, Eq. (31)] and the sharp reduction in power at multipoles greater than a few thousand is effectively due to the decrease in primary anisotropy power at small angular scales. In the case of the lensing-secondary correlation, the trispectrum is only proportional to one power of the CMB anisotropy power spectrum. Thus, the trispectrum now depicts more of the behavior of the lensing-secondary correlation power spectrum shown in Fig. 2. The sharp decrease in the lensing-ISW trispectrum compared to that of the lensing-SZ effect is due to differences in the small angular scale power associated with lensing-ISW and lensing-SZ correlations.

We can now use this trispectrum to study the contributions to the covariance. In Fig. 4, we show the ratio of the

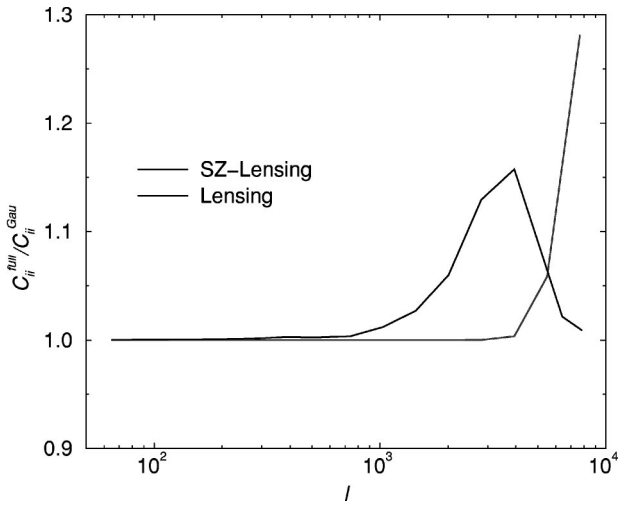

FIG. 4. The ratio of full variance, including non-Gaussian covariance, to that when non-Gaussian trispectrum contributions are neglected. This ratio shows the fractional change in the variance, or the errors along the diagonal of the covariance matrix. Out to multipoles of a few thousand, the increase due to lensing is less than few percent and at the smallest scale there is no change from the lensing alone trispectrum as its contributions are substantially small. The lensing-SZ trispectrum only makes noticeable contributions at the smallest scale. The resulting changes from the lensing-ISW trispectrum is below 10^{-6} and can be ignored.

diagonal of the full covariance to the Gaussian variance with the non-Gaussian term neglected:

$$R \equiv \frac{C_{ii}}{\mathcal{C}_i}, \tag{41}$$

and for bands l_i given in Table I. Here, we have used rather wide bins in multipoles such that bin width is constant in logarithmic intervals in multipole space. This is the same binning scheme used by Ref. [41] on $6^\circ \times 6^\circ$ fields to investigate weak lensing covariance and later adopted by Ref. [17]. The two lines show the ratio when trispectra due to lensing and lensing-SZ correlations are used to calculate the covariance, respectively. The square root of the ratio is roughly the fractional change induced in errors along the diagonal resulting from the non-Gaussian covariance contributions. We do not show the ratio due to lensing-ISW trispectrum as the resulting changes are less than 10^{-6} at all multipoles of interest. As shown in Fig. 4, the ratio is less than 20% for weak lensing and peaks at multipoles ~ 4000 while the ratio increases to smallest scale with the lensing-SZ trispectrum.

The correlation between the bands is given by

$$\hat{C}_{ij} \equiv \frac{C_{ij}}{\sqrt{C_{ii}C_{jj}}}. \tag{42}$$

In Table I we tabulate the correlation coefficients for the CMB binned power spectrum measurements. The upper triangle here are the correlations under the lensing trispectrum while the lower triangle shows the correlations found with the trispectrum due to lensing-SZ correlations. In the case of lensing contribution to the trispectrum, correlations depict the general shape of the CMB power spectrum while in the case of lensing-SZ contribution to the covariance, the correlation coefficients are more consistent with the shape of the lensing-SZ power spectrum.

In Fig. 5, we show the correlation coefficients for (a) lensing and (b) lensing-SZ contributions to the covariance. Here we show the behavior of the correlation coefficient between a fixed l_j (as noted in the figure) as a function of l_i. Note that when $l_i = l_j$ the coefficient is 1 by definition; we have not included this point in the figure due to the apparent discontinuity it creates from the dominant Gaussian contribution at $l_i = l_j$.

To better understand how the non-Gaussian contributions scale with our assumptions, we consider the ratio of non-Gaussian variance to the Gaussian variance (see Refs. [16,17])

$$\frac{C_{ii}}{C_{ii}^G} = 1 + R, \tag{43}$$

TABLE I. Weak lensing convergence power spectrum correlations. Upper triangle displays the covariance with the lensing trispectrum alone, while the lower triangle (parenthetical numbers) displays the covariance with the trispectrum due to lensing-SZ correlation. We do not tabulate the covariance due to trispectrum resulting from lensing-ISW correlation as the correlation coefficients are of order 10^{-6} or below. The data are binned such that bin sizes are constant in logarithmic intervals.

$l_{\rm bin}$	529	739	1031	1440	2012	2812	3930	5492	7674
529	1.000	0.002	0.002	0.003	0.005	0.013	0.059	0.239	0.554
739	(0.000)	1.000	0.010	0.007	0.009	0.021	0.091	0.348	0.783
1031	(0.000)	(0.000)	1.000	0.013	0.012	0.025	0.090	0.318	0.686
1440	(0.000)	(0.000)	(0.000)	1.000	0.025	0.034	0.093	0.277	0.547
2012	(0.000)	(0.000)	(0.000)	(0.000)	1.000	0.060	0.092	0.200	0.336
2812	(0.000)	(0.000)	(0.000)	(0.000)	(0.000)	1.000	0.101	0.102	0.125
3930	(0.000)	(0.000)	(0.000)	(0.000)	(-0.001)	(-0.002)	1.000	0.039	0.021
5492	(0.000)	(0.001)	(0.000)	(0.000)	(-0.001)	(-0.005)	(-0.031)	1.000	0.001
7674	(0.000)	(0.001)	(0.000)	(0.000)	(0.000)	(-0.001)	(-0.016)	(-0.186)	1.000

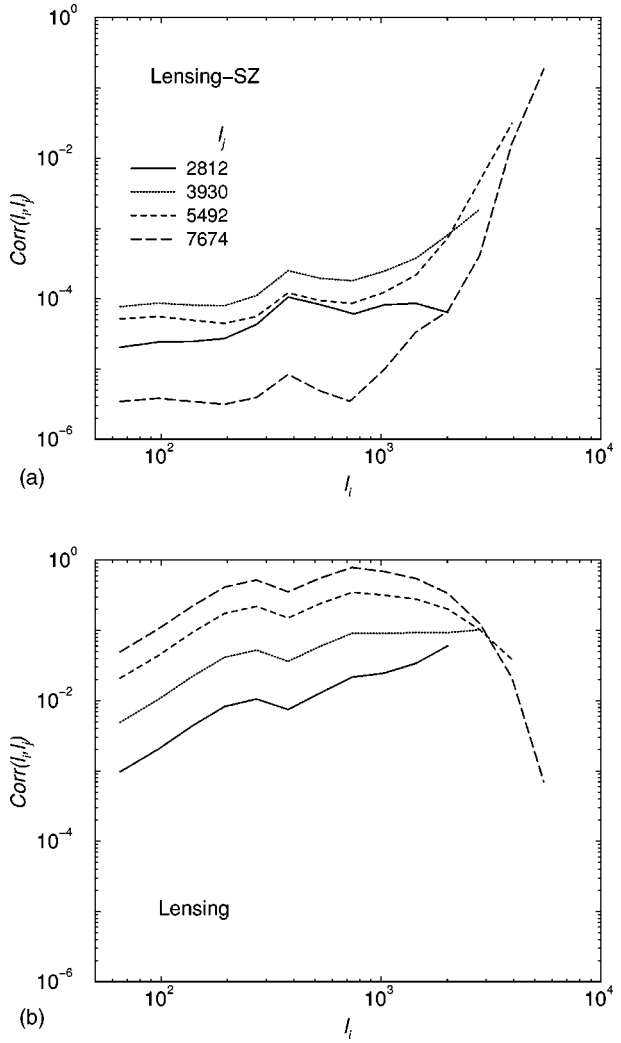

FIG. 5. The correlation coefficients of (a) lensing and (b) lensing-SZ contributions to the covariance of the CMB angular power spectrum. In the case of the lensing, the correlations show the general behavior of the lensing effect on CMB where power is transferred from large angular scales with acoustic peaks to small angular scales, thereby correlating small and large angular scales at the tens of percent level or more. For experiments such as Planck, that will measure the power spectrum to multipoles of ~ 2000, the resulting correlations between bins are less than a percent.

with

$$R \equiv \frac{A_{si} T^{\Theta}_{ii}}{(2\pi)^2 2 C_i^2}. \tag{44}$$

In the case of the lensing alone contribution to CMB trispectrum, we can simplify the expression for R by noting that

$$T^{\Theta}(\mathbf{l}_i, -\mathbf{l}_i, \mathbf{l}_j, -\mathbf{l}_j)|_{l_i = l_j} \sim 8 C^{\Theta}_{l_i} C^{\Theta}_{l_i} C^{\phi\phi}_{\sqrt{2} l_i} l_i^4, \tag{45}$$

where for an approximation we have taken $\mathbf{l}_i \cdot \mathbf{l}_j = 0$. Replacing the averaging of the product of $(C^{\Theta}_{l_i})^2 C^{\phi\phi}_{l_i}$ with the product of two averages, we can simplify the ratio of T^{Θ}_{ii}/C_i^2 to obtain

$$R \sim 4 l_i \delta l_i \left\langle \frac{l_i^4 C^{\phi\phi}_{l_i}}{2\pi} \right\rangle_{A_i}, \tag{46}$$

where $\langle \cdots \rangle_{A_i}$ represents the averaging of the lensing potential power spectrum, weighted by a factor of l_i^4 to represent the deflection angles. Equation (46) represents the general behavior of the non-Gaussian contribution to the lensing trispectrum. The relative contributions from non-Gaussianities scale with several parameters: (a) increasing the bin size, through $\delta l_i (\propto A_{si})$, leads to an increase in the non-Gaussian contribution linearly while (b) the contribution is determined by the shape of the lensing potential power spectrum, weighted by a factor of l_i^2, which accounts for the angular gradients in the deflection angle. At large multipoles, beyond l's of few thousand, the potential power spectrum in Fig. 2(a) drops rapidly leading to a decreases in the non-Gaussian contribution and thus to the covariance of CMB temperature anisotropy. The fact that the lensing potential power spectrum is not significant at multipoles of thousand is somewhat contrary to the general assumption that lensing is a small angular scale phenomenon restricted to arcminutes or less. In the case of CMB angular deflections, the rms deflection angle of a CMB photon due to large scale structure is roughly 2.6 arcmins with a coherence of roughly 10 ° [43]. Thus, lensing of CMB can be effectively considered as an arcminute to degree scale effect instead of arcsecond scales typically encountered in conventional gravitational lensing with galaxies and quasars.

For upcoming wide-field experiments, especially those involving satellite missions such as MAP and Planck, we do not expect non-Gaussianities to limit the interpretation and the cosmological parameter extraction from the measured CMB power spectrum. For these wide-field experiments, the width of the bin in multipole space will be of order at most few tens; for such small bin widths in multipole space at $l \sim$ few hundred will lead to a significantly reduced ratio of non-Gaussian to Gaussian contribution from what we have considered where $\delta l \sim l$. Also, note that the cosmologically interesting acoustic peak structure and the damping tail of the CMB anisotropies is limited to multipoles below ~ 1000. In this range, there is no significant non-Gaussian contribution related to lensing and lensing-secondary correlations.

There are, however, ground-based experiments (e.g., Cosmic Background Imager [20]) for which the non-Gaussianities due to lensing may be important. These small angular scale experiments, which probe the anisotropy power between multipoles of ~ 1000 and 4000 or so are likely to be limited to small areas on the sky and will utilize wide bins in multipole space when estimating the power spectrum in order to increase the signal-to-noise associated with its measurement. In such a scenario, it may be necessary to fully account for the full covariance when interpreting the power spectrum at small angular scales. In the absence of many fields where the covariance can be estimated directly from the data, the analytical calculations provide a useful quantification of the covariance. Such an analytical approach, however, requires *a priori* knowledge of cosmology and details

regarding, say, clustering of large scale structure pressure that is responsible for the SZ effect.

As a practical approach, one could imagine taking the variances estimated from the survey under a Gaussian approximation, but which accounts for effects related to windowing, and scaling it up by the non-Gaussian to Gaussian variance ratio with an analytical calculation along with inclusion of the band power correlations. Additionally, it is in principle possible to use the expected correlations due to non-linear mode coupling effects such as lensing to decorrelate individual band power measurements (e.g., Ref. [44]).

VI. SUMMARY

The upcoming small angular scale CMB anisotropy experiments are expected to provide first measurements of the power spectrum related to the damping tail and secondary anisotropies. At such scales, important non-linear effects and secondary contributions can imprint non-Gaussian signals on the CMB temperature fluctuations. Here, we discussed one aspect related to the presence of non-Gaussianities when measuring the CMB anisotropy power spectrum involving a contribution to the covariance resulting from the higher order four-point correlation function, or a trispectrum in Fourier space. Here, we discussed the non-Gaussian contribution to the power spectrum covariance of CMB anisotropies resulting through weak gravitational lensing angular deflections and the correlation of deflections with the integrated Sachs-Wolfe effect and the Sunyaev-Zel'dovich effect.

The covariance due to the lensing effect on CMB alone is significant at multipoles ~ 1000 while the lensing-SZ correlation dominates at multipoles above ~ 4000 corresponding to observations at angular scales of arcminutes or less. The covariance due to lensing-ISW correlation peaks at large angular scales, as the ISW effect peaks at low multipoles, and can effectively be considered negligible due to the dominant Gaussian sample variance at such low multipoles. With substantially wide bins in multipole space, the resulting non-Gaussian contribution from lensing to the binned power spectrum variance is insignificant out to multipoles of few thousand containing acoustic peaks and the damping tail, which are of substantial interest for cosmological parameter estimation purposes.

For a experiment like MAP, sensitive to multipoles out to ~ 800, the lensing effect only increases the variance by $\sim 0.05\%$ relative to the Gaussian variance, while for Planck, the non-Gaussian nature of lensing increases the variance, relative to the Gaussian variance, by 4% at multipoles of ~ 1500. Thus, for these satellite based near all-sky experiments, we do not expect non-Gaussianities to limit the cosmological parameter extraction from CMB power spectrum measurements and their interpretation. For small angular scale ground-based experiments with substantially limited sky coverage, however, the presence of non-Gaussianities should be accounted for when interpreting any measurements at angular scales corresponding to few arcminutes or multipoles ~ 4000. Such an ongoing experiment is the Cosmic Microwave Background Imager [20], while similar experiments are planned or are underway based on interferometric and bolometric techniques. Here, the non-Gaussian nature of lensing increases the power spectrum variance up to 15% at multipoles of ~ 4000. Even if the SZ effect is removed from CMB data, the lensing effect alone produces a significant non-Gaussianity at arcminute scales and cannot be simply ignored for precision work related to cosmology or astrophysics.

ACKNOWLEDGMENTS

We acknowledge support from the Sherman Fairchild Foundation and from the U.S. DOE Grant No. D.E.-FG03-92-ER40701.

[1] P. J. E. Peebles and J. T. Yu, Astrophys. J. **162**, 815 (1970); R. A. Sunyaev and Ya. B. Zel'dovich, Astrophys. J. **7**, 3 (1970); J. Silk, Astron. Astrophys., Suppl. Ser. **151**, 459 (1968); see recent review by W. Hu and S. Dodelson, Annu. Rev. Astro. (to be published), astro-ph/0110414.

[2] L. Knox, Phys. Rev. D **52**, 4307 (1995); G. Jungman, M. Kamionkowski, A. Kosowsky, and D. N. Spergel, *ibid.* **54**, 1332 (1996); J. R. Bond, G. Efstathiou, and M. Tegmark, Mon. Not. R. Astron. Soc. **291**, L33 (1997); M. Zaldarriaga, D. N. Spergel, and U. Seljak, Astrophys. J. **488**, 1 (1997); D. J. Eisenstein, W. Hu, and M. Tegmark, *ibid.* **518**, 2 (1999).

[3] A. Blanchard and J. Schneider, Astron. Astrophys. **184**, 1 (1987); A. Kashlinsky, Astrophys. J. Lett. **331**, L1 (1988); E. V. Linder, Astron. Astrophys. **206**, 1999 (1988); S. Cole and G. Efstathiou, Mon. Not. R. Astron. Soc. **239**, 195 (1989); M. Sasaki, *ibid.* **240**, 415 (1989); K. Watanabe and K. Tomita, Astrophys. J. **370**, 481 (1991); M. Fukugita, T. Futumase, M. Kasai, and E. L. Turner, *ibid.* **393**, 3 (1992); L. Cayon, E. Martinez-Gonzalez, and J. Sanz, *ibid.* **413**, 10 (1993); U. Seljak, *ibid.* **463**, 1 (1996).

[4] D. N. Spergel and D. M. Goldberg, Phys. Rev. D **59**, 103001 (1999); D. M. Goldberg and D. N. Spergel, *ibid.* **59**, 103002 (1999); M. Zaldarriaga and U. Seljak, *ibid.* **59**, 123507 (1999); H. V. Peiris and D. N. Spergel, Astrophys. J. **540**, 605 (2000).

[5] A. Cooray and W. Hu, Astrophys. J. **534**, 533 (2000).

[6] W. Hu, Phys. Rev. D **64**, 083005 (2001).

[7] K. Benabed, F. Bernardeau, and L. van Waerbeke, Phys. Rev. D **63**, 043501 (2001); J. Guzik, U. Seljak, and M. Zaldarriaga, *ibid.* **62**, 043517 (2000); M. Zaldarriaga and U. Seljak, *ibid.* **58**, 023003 (1998).

[8] A. Gangui, F. Lucchin, S. Matarrese, and S. Mollerach, Astrophys. J. **430**, 447 (1994); G. Hinshaw, A. J. Banday, C. L. Bennett, K. M. Gorski, and A. Kogut, *ibid.* **446**, 67 (1995); P. G. Ferreira, J. Magueijo, and K. M. Gorski, *ibid.* **503**, 1 (1998).

[9] E. Komatsu and D. N. Spergel, Phys. Rev. D **63**, 063002 (2001); L. Wang and M. Kamionkowski, *ibid.* **61**, 063504 (1999); A. Gangui and J. Martin, Mon. Not. R. Astron. Soc. **313**, 323 (2000); X. Luo and D. N. Schramm, Phys. Rev. Lett. **71**, 1124 (1994); X. Luo, Astrophys. J. **427**, 71 (1994); T. Falk,

R. Rangarajan, and M. Frednicki, Astrophys. J. Lett. **403**, L1 (1993).
[10] R. A. Sunyaev and Ya. B. Zel'dovich, Mon. Not. R. Astron. Soc. **190**, 413 (1980).
[11] A. Cooray, Phys. Rev. D **64**, 043516 (2001).
[12] A. Cooray, W. Hu, and M. Tegmark, Astrophys. J. **540**, 1 (2000).
[13] F. Bernardeau, Astron. Astrophys. **324**, 15 (1997).
[14] W. Hu, Phys. Rev. D **62**, 043007 (2000).
[15] M. Zaldarriaga, Phys. Rev. D **62**, 063510 (2000).
[16] R. Scoccimarro, M. Zaldarriaga, and L. Hui, Astrophys. J. **527**, 1 (1999); D. J. Eisenstein and M. Zaldarriaga, *ibid.* **546**, 2 (2001).
[17] A. Cooray and W. Hu, Astrophys. J. **554**, 56 (2001).
[18] R. K. Sachs and A. M. Wolfe, Astrophys. J. **147**, 73 (1967).
[19] J. E. Carlstrom, M. Joy, and L. Grego, Astrophys. J. Lett. **456**, L75 (1996); M. Jones *et al.*, Nature (London) **365**, 320 (1993).
[20] S. Padin *et al.*, astro-ph/0110124.
[21] A. Cooray, Phys. Rev. D **64**, 063514 (2001); Ph.D. thesis, University of Chicago, Chicago, 2001, avilable from the University of Chicago Crear Science Library or from the author.
[22] N. Kaiser, Astrophys. J. **388**, 286 (1992); N. Kaiser, *ibid.* **498**, 26 (1998); M. Bartelmann and P. Schneider, Phys. Rep. **340**, 291 (2001).
[23] D. Limber, Astrophys. J. **119**, 655 (1954).
[24] J. M. Bardeen, Phys. Rev. D **22**, 1882 (1980).
[25] D. J. Eisenstein and W. Hu, Astrophys. J. **511**, 5 (1999).
[26] E. F. Bunn and M. White, Astrophys. J. **480**, 6 (1997).
[27] P. T. P. Viana and A. R. Liddle, Mon. Not. R. Astron. Soc. **303**, 535 (1999).
[28] P. J. E. Peebles, *The Large-Scale Structure of the Universe* (Princeton University Press, Princeton, 1980).
[29] J. A. Peacock and S. J. Dodds, Mon. Not. R. Astron. Soc. **280**, L19 (1996).
[30] P. Valageas, Astron. Astrophys. **354**, 767 (2000).
[31] U. Seljak and M. Zaldarriaga, Phys. Rev. D **60**, 043504 (1999).
[32] M. Takada and N. Sugiyama, astro-ph/0110313.
[33] J. P. Ostriker and E. T. Vishniac, Nature (London) **322**, 804 (1986); E. T. Vishniac, Astrophys. J. **322**, 597 (1987); S. Dodelson and J. M. Jubas, *ibid.* **439**, 503 (1995); G. Efstathiou, in *Large Scale Motions in the Universe. A Vatican Study Week*, edited by V. C. Rubin and G. V. Coyne (Princeton University Press, Princeton, 1988), p. 299; A. H. Jaffe and M. Kamionkowski, Phys. Rev. D **58**, 043001 (1998); W. Hu, Astrophys. J. **529**, 12 (1999).
[34] A. Cooray, Phys. Rev. D **62**, 103506 (2000).
[35] U. Seljak, Mon. Not. R. Astron. Soc. **318**, 203 (2000); C.-P. Ma and J. N. Fry, Astrophys. J. Lett. **538**, L107 (2000); R. Scoccimarro, R. Sheth, L. Hui, and B. Jain, Astrophys. J. **546**, 20 (2001); A. Cooray, W. Hu, and J. Miralda-Escude, Astrophys. J. Lett. **536**, L9 (2000); A. Cooray and R. K. Sheth, Phys. Rep. (to be published).
[36] W. H. Press and P. Schechter, Astrophys. J. **187**, 425 (1974); see, also, R. K. Sheth and B. Tormen, Mon. Not. R. Astron. Soc. **308**, 119 (1999).
[37] J. Navarro, C. Frenk, and S. D. M. White, Astrophys. J. **462**, 563 (1996); B. Moore, T. Quinn, F. Governato, J. Stadel, and G. Lake, Mon. Not. R. Astron. Soc. **310**, 1147 (1999).
[38] H. J. Mo, Y. P. Jing, and S. D. M. White, Mon. Not. R. Astron. Soc. **284**, 189 (1997); H. J. Mo and S. D. M. White, *ibid.* **282**, 347 (1996).
[39] A. Refregier and R. Teyssier, astro-ph/0012086.
[40] U. Seljak and M. Zaldarriaga, Astrophys. J. **469**, 437 (1996).
[41] M. White and W. Hu, Astrophys. J. **537**, 1 (1999).
[42] U. Seljak and M. Zaldarriaga, Astrophys. J. **538**, 57 (2000).
[43] W. Hu and A. Cooray, Phys. Rev. D **63**, 023504 (2000).
[44] A. J. S. Hamilton, Mon. Not. R. Astron. Soc. **289**, 285 (1997); A. J. S. Hamilton and M. Tegmark, *ibid.* **312**, 285 (2000).